SECTION 4

ARTS-IIIA SIGNAL PROCESSING

INTRODUCTION

This section considers the effects of asynchronous pulse interference on the FAA ARTS-III Enhancement signal processing and its impact on the radar's probability of detection and false alarm. The Automated Radar Terminal System (ARTS) III processor presently employed at terminal radar control facilities utilizes flight plan information from Air Route Traffic Control Centers (ARTCC) and Air Traffic Control Beacon Interrogator (ATCBI) video. In addition to providing target reports on transponder aircraft, alphanumeric data blocks available for display are continually associated with the appropriate aircraft targets by a tracking program. The primary or radar video is not processed by the present ARTS-III system. The ARTS-III enhancement, referred to as the ARTS-IIIA, processes the video target information from both the Airport Surveillance Radars (ASR) and the ATCRBS. The ARTS-IIIA consists of a Radar Data Acquisition Subsystem (RDAS), Beacon Data Acquisition Subsystem (BDAS), and a Common Processor Subsystem (CPS). Primary radar inputs are processed by the RDAS to produce radar reports and weather map data, and the beacon inputs are processed by the BDAS to produce beacon reports. The CPS correlates radar and beacon reports and transmits target and weather reports. Interference effects on the RDAS only are considered in this report since it is the portion of the ARTS-IIIA which processes the 2.7 to 2.9 GHz radar signals.

The ARTS-IIIA is currently scheduled to be operationally deployed at 60 airports throughout the United States. This is a substantial deployment since it involves over 25 percent of the FAA Radar equipped airports in the U.S. The first ARTS-IIIA operational deployment is scheduled for July 1979 at Minneapolis, Minnesota. The deployment at each of the remaining 59 locations is scheduled at every two-month interval after this initial date.

RADAR DATA ACQUISITION SUBSYSTEM DESCRIPTION

The RDAS is designed to receive analog video signals from the ASR-4, 5, 6, 7, and ARSR-2 radar or digital signals from the ASR-8 or ARSR-3. Provisions are made in the RDAS design for processing analog or digital video input by a printed circuit board insertion. The function of the RDAS is to detect and report aircraft and clutter derived from the search radar. The RDAS, as illustrated in Figure 4-1, consists of two functional units, referred to as the Radar Extractor (REX) and the Radar Microcontroller (RMC). The RDAS/REX simultaneously accepts normal, MTI, and synchronizing signals from the radar receiver.

The REX performs target detection and clutter monitor functions, and provides target reports and clutter counts to the RMC. The RMC employs these

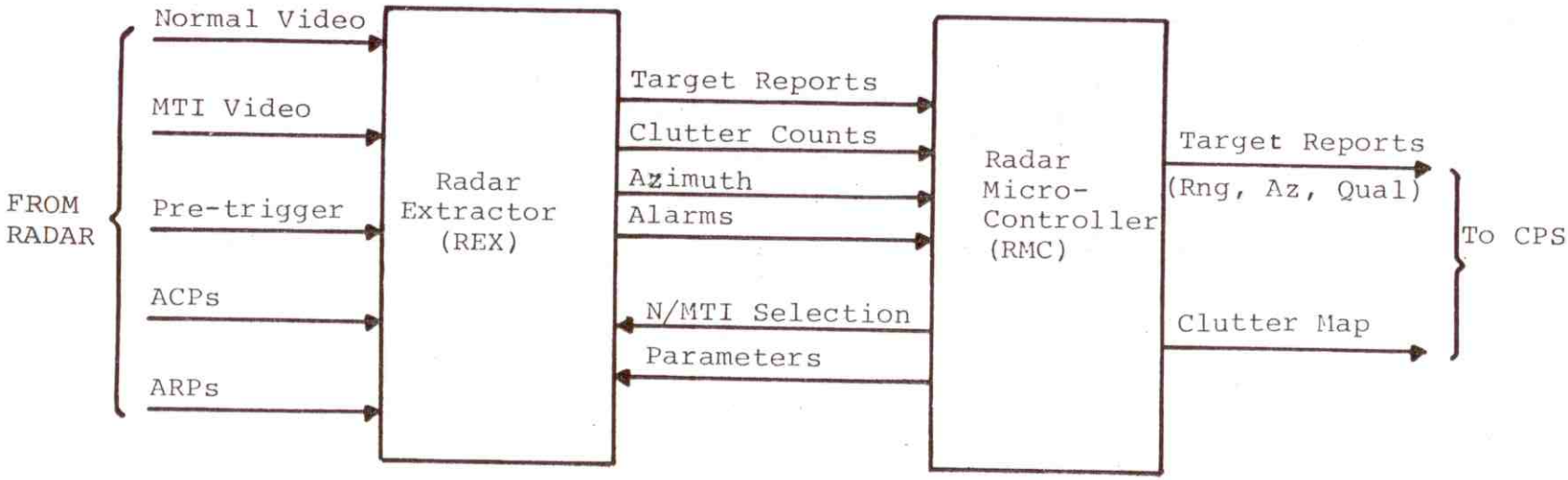

Figure 4-1. Block Diagram of Radar Data Acquisition Subsystem

clutter counts to determine the type video (normal or MTI) and MTI target detection threshold for optimum target detection performance. The video select and MTI threshold control signals from the RMC are fed back to the REX. The RDAS/RMC output provides target reports, including target range, azimuth, and report quality, to the Common Processing Subsystem (CPS). A two level clutter map is also provided to the CPS for indication of weather conditions.

A functional description of the REX and RMC follows. Only those control functions will be discussed that have a bearing on the interference analysis.

Radar Extractor

A simplified block diagram of the Radar Extractor (REX) is shown in Figure 4-2. The function of each unit in the signal flow path will be briefly described in this subsection.

Video Multiplexer Converter

The video multiplexer converter transforms the MTI and normal video received from the radar into a multiplexed serial digital bit stream. The multiplexer converter includes analog to digital converters when the RDAS is interfaced with ASR-4, 5, 6 and 7 analog video radars. When the RDAS is interfaced with the frequency diversity ASR-8 radar, in which both frequency channels are simultaneously operated, one sample per range bin from each channel are received by the REX multiplexer converter.

Rank Order Detection Process

The ARTS-IIIA employs a rank order detection process to detect target hits or pulse returns. The rank order detection process is performed by the Rank Quantizer and Hit Processor (see Figure 4-2). Rank order detection is a binary detection concept that utilizes a nonparametrical statistical decision process. That is, the rank order detector has a distribution free property in which the probability of a 1 being generated when no target is present (probability of false target hit) is independent of the noise or clutter distribution if the samples are from an identical probability distribution and statistically independent. Under these conditions the rank order detector yields a constant false alarm rate regardless of the environmental clutter level. The operation of the rank order detector involves comparing the amplitude sample of the range or target bin of interest with the sampled noise and clutter levels in adjacent range bins over each Azimuth Change Pulse (ACP). The number of cases that the amplitude of the target sample exceeds adjacent range samples is defined as the rank of the target sample. If this rank exceeds or equals a rank threshold, a target hit (logical 1) is generated, otherwise a miss (logical 0) is generated.

Rank Quantizer. The rank quantizer portion of the REX (see Figure 4-2) computes the rank of the range bin, and the hit processor unit compares this rank with a threshold to determine if a target hit has occurred. A

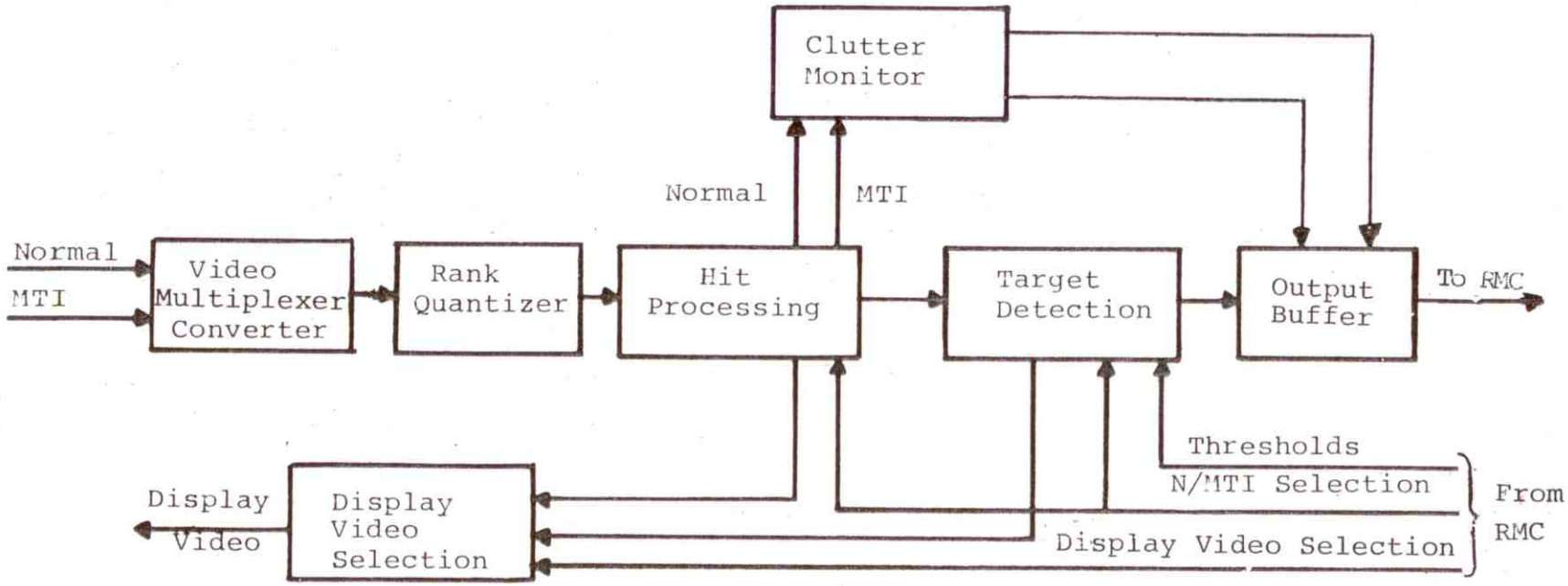

Figure 4-2. Block Diagram of Radar Extractor

simplified block diagram of the rank quantizer portion of the rank order detector is shown in Figure 4-3. The digital range bin samples enter a 27 stage shift register, in which delays between adjacent shift register stage taps correspond to the time resolution of the range bins. The signal amplitude in the range bin of interest (S14) from the center tap of the shift register is compared with the signal amplitude (usually noise) in the range bins before (S1-S12) and after (S16-S27) the range bin of interest. Signal samples from range bins S13 and S15 immediately adjacent to the range bin of interest are not compared with the range bin of interest to prevent long target pulses from overlapping both target and adjacent range bins and being interpreted as noise samples. The comparators (C_i) associated with each range bin outputs a one if the signal in the bin of interest (S14) is greater than the compared to range bin (S1-S12 and S16-S27). The comparator outputs are summed to obtain a rank (0-24) of the range bin of interest. It should be pointed out that the actual rank quantizer utilized in the REX is slightly more complicated than that indicated in Figure 4-3, because the rank quantizing processing is performed on a serial stream of interlaced normal and MTI bits. However, the logic depicted in Figure 4-3 is identical for both the normal and MTI channels.

Hit Processor. The block diagram of the hit processing logic is shown in Figure 4-4. The input consists of a five bit rank value from the rank quantizer. The rank data is processed simultaneously in two paths to produce target and clutter hits respectively. If the rank value in the upper path equals or exceeds a rank quantizer threshold (typically 23 or 24) a target hit is generated and a logical 1 assigned to the range bin of interest. That is, if the signal amplitude in the range bin of interest has exceeded the voltage level in all but one of the 24 adjacent reference range bins or all 24 of the adjacent reference range bins, depending on which rank quantizer threshold setting is used, a target hit is generated. If the rank does not exceed the rank quantizer threshold, a miss is generated and a logical 0 assigned to the range bin of interest. In the lower path (see Figure 4-4), if the rank exceeds or equals a rank quantizer threshold of 17, a clutter hit is generated and a logical 1 assigned to the range bin of interest. In other words, for a clutter hit to be declared the signal amplitude in the range bin of interest has to exceed 17 of the 24 adjacent sample range bins. This rank quantizer threshold testing in the upper and lower channel of the hit processor provides the last phase in the rank order detection process. Both the target and clutter hit paths include demultiplexers after the rank quantizer threshold comparators to separate out the normal and MTI digital signals. The normal or MTI target hits are selected for further target detection processing by a feedback control signal from the RMC. The selection is based on the normal clutter hit data provided by the hit processing logic. Basically, normal is selected in light clutter and MTI in heavy clutter conditions. A normal or MTI video selection is made for each 32 azimuth change pulse (ACP) by 32 range bin (RB) zone. This represents approximately a 2.8 degree by 2 nmi zone. The normal and MTI clutter hit information used for the normal/MTI target hit selection is routed to the RMC through the clutter monitor unit and output buffer (see Figure 4-2).

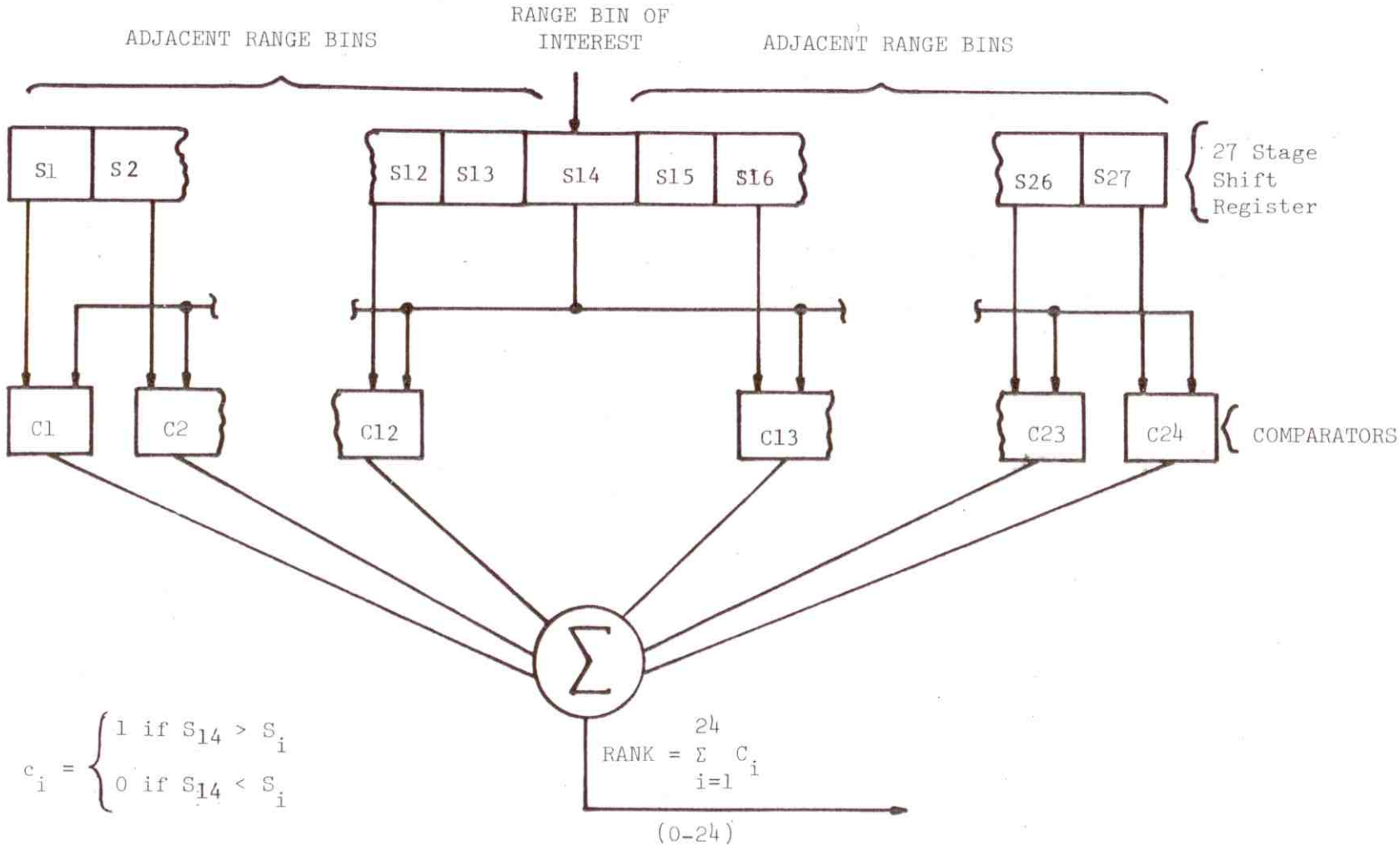

Figure 4-3. Block Diagram of Rank Quanitzer Logic

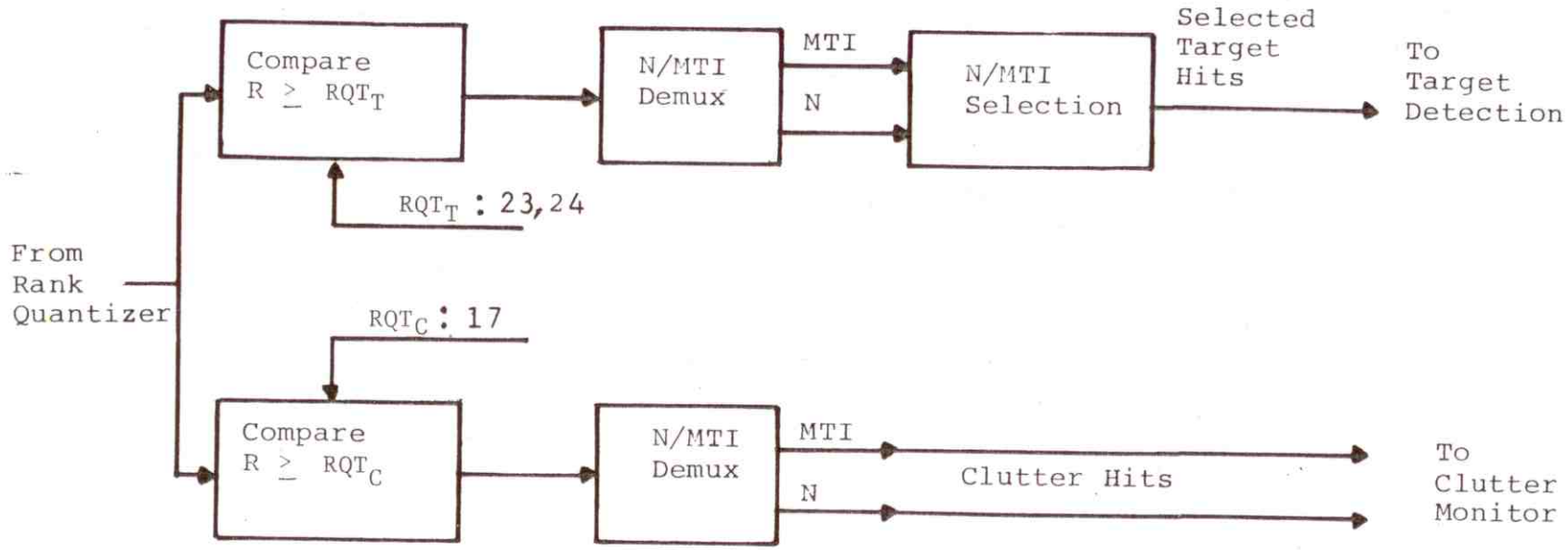

Figure 4-4. Block Diagram of Hit Processing Logic

Target Detection

The target detection stage in the REX is shown in Figure 4-2 and the details of the software functions in Figure 4-5. The target detection software logic first correlates the hit and miss data received from the hit processor unit with the appropriate range bins. A record of the target hits (1) and misses (0) in azimuth for a given range bin is initialized and maintained when a target hit is generated. When the consecutive misses (zeros) in the record equals or exceeds a miss count threshold (typically 3 or 4), the accumulated sum of the target hits since the beginning of the record is examined. If the target hit count equals or exceeds the hit count threshold, a target is declared. For the normal radar channel the target hit count threshold is fixed (typically at 8 or 9) and the MTI channel is variable. The MTI hit target count threshold is increased from the normal channel threshold value up to 20 depending on the degree of pulse-to-pulse correlation of the clutter. When a target is declared, the hit/miss record is terminated. The record is also terminated under the following two conditions:

(1) The miss count threshold is exceeded but the hit count threshold is not.

(2) The record length (number of ACPs) reaches 30 and the consecutive miss count and hit count threshold are not satisfied.

The target hit/miss record is extended beyond 30 ACPs if the hit count threshold is satisfied, but the miss count threshold is not. In this case, the hit and consecutive miss count is continued until the target detection or record termination criteria is met.

Clutter Monitor Logic

The function of the clutter monitor logic, shown in Figures 4-2 and 4-6, is to count "isolated hits" over 32 range bin (RB) blocks in both the normal and MTI channel, and output these counts to the RMC. Isolated hits are those preceded and followed by a miss (010 pattern) over a 3 ACP (pulse transmission) sequence in azimuth at a fixed range. The "isolated hits" (010 hit/miss pattern) are detected by the 3 stage shift register, inverters, and "and gate" logic shown in each video channel in Figure 4-6. The counters following the "and gate" count the number of isolated hits that occur over the 32 RB's. If more than 15 isolated hits occur in a 32 RB interval, a maximum count of 15 is outputted.

Radar Micro Controller

The Radar Micro Controller (RMC) is a digital data processing device that uses a microprogrammed control structure, involving microinstructions and control data stored in a read only memory (ROM). This RMC firmware controls the data flow between the REX and RMC and formats the RDAS output data. The RMC receives normal and MTI channel Isolated Hit Sum (IHS) data

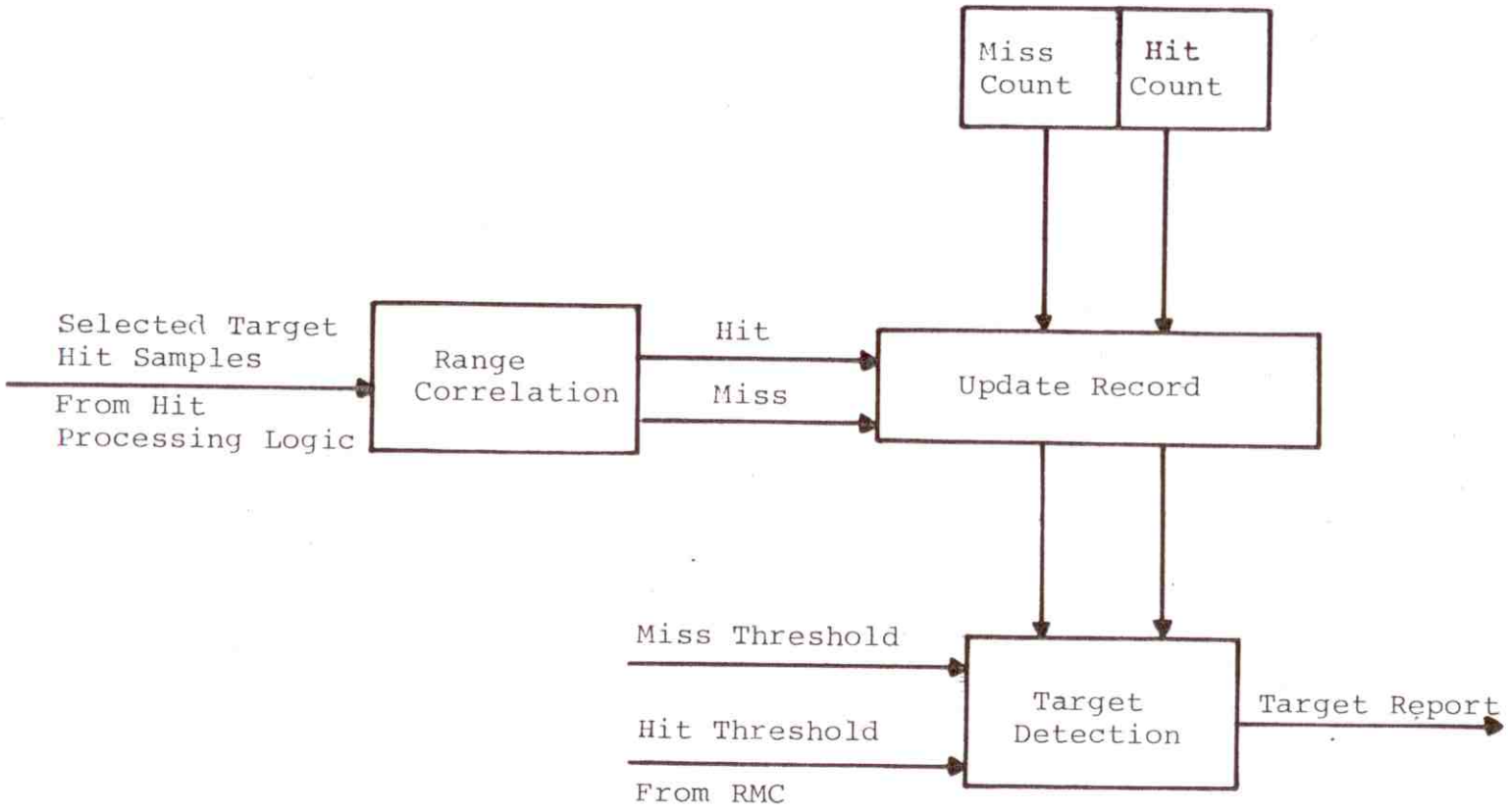

Figure 4-5 Block Diagram of Target Detection

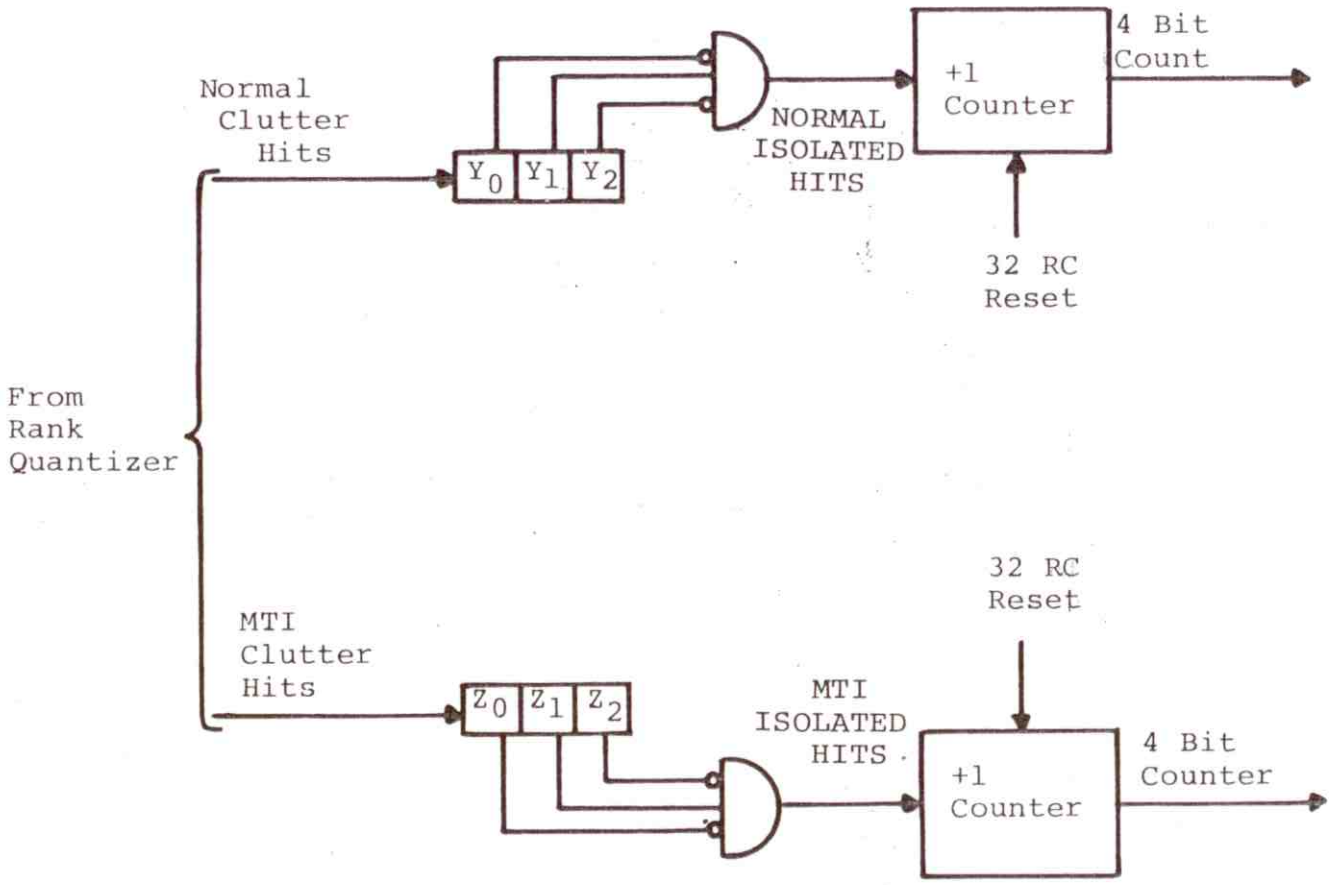

Figure 4-6 Block Diagram of Clutter Monitor Logic

from the REX clutter monitor. The normal channel IHS clutter data is used by the RMC to select the optimum video (normal or MTI) for target detection processing, and the MTI channel IHS clutter data to adjust the MTI target detection criteria (target hit count threshold). The first paragraph below discusses the RMC control processing associated with the video selection, and the second paragraph the RMC control processing associated with the MTI target detection threshold control.

The RMC receives normal channel IHS clutter data in 32 RB blocks and forms a clutter map of IHS's in 32 RB by 32 ACP zones. The sum of the normal video isolated hits for the zone on the previous antenna scan is used to update a clutter zone on the current antenna scan. The magnitude of the updated clutter count represents the level of clutter returns and is used to derive the video select command for the zone. The following criteria is used to update the zone clutter count and arrive at a video select decision. If the IHS for the 32 RB x 32 ACP zone on the previous antenna scan is greater than a variable clutter count threshold (typically 166), the clutter count shall be incremented by 1. If the IHS is less than or equal to this threshold value, the clutter count is decremented by 1. If the resulting clutter count exceeds 7, the MTI channel is selected. Conversely, if the clutter count is less than or equal to 7, the normal channel is selected. Basically normal video is selected in light or zero clutter zones, and MTI video is selected in heavy clutter zones.

When MTI video has been selected, the RMC controls the MTI video target hit threshold to maintain a constant false alarm rate. Unlike noise hits, the amplitude of pulse-to-pulse clutter returns are often correlated which results in a higher probability of false alarm. The rank order detection process is only partially effective in maintaining a constant false alarm rate for these conditions, since it only accounts for first order statistics (average number of independent hits) of the clutter distribution. The RMC uses the MTI channel clutter IHS measured by the clutter monitor logic to determine the degree of pulse-to-pulse correlation. The RMC maintains a 32 RB (2 nmi) by 32 ACP (2.8 degrees) sliding window of MTI cumulative IHS. The 32 RB blocks of MTI channel IHS received from the clutter monitor logic are added to the sliding window's cumulative sum, and the 32 RB block IHS received 32 ACPs before subtracted. The current sliding window cumulative sum is used to derive the MTI channel target hit count threshold. The target hit count threshold is linearly increased from the normal channel threshold value with decreasing values of sliding window IHS's in the manner indicated in Figure 4-7. This type of functional control tends to maintain a constant false alarm by increasing the hit count threshold for a high pulse-to-pulse amplitude correlated clutter or equivalently a low IHS count.

ARTS-IIIA RDAS INTERFERENCE ANALYSIS

The ARTS-IIIA RDAS interference analysis involved determining the effect of radar asynchronous interference on the victim radar's probability of false alarm and target detection. This involved applying a combination of analytical and simulation techniques.

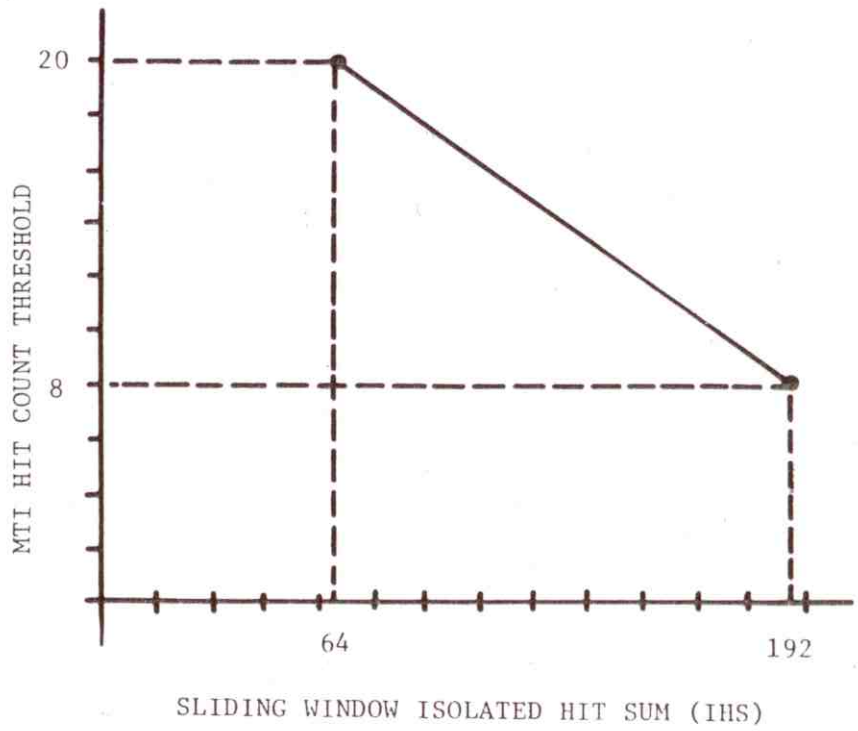

Figure 4-7. ARTS-IIIA/RDAS MTI Channel Hit Count Threshold Control for Maintaining a Constant False Alarm Rate

In particular, the effect of interference on the probability of a false target hit and target hit detection was defined analytically for worst-case interference signal level conditions, and then related to probability of false alarm and target detection by simulation of the processors target detection criteria. This method of analysis was performed for all combinations of ARTS-IIIA/RDAS target detection parameters so that trade-offs between interference suppression and radar performance could be investigated. The effect of interference on the ARTS-IIIA/RDAS automatic video selection and MTI hit count threshold control was analyzed using statistical and probability theory. Those interference and target signal level conditions which maximized the effect of interference were assumed in the analysis. This worst-case approach allowed analytical techniques to be employed instead of the more time consuming complete ARTS-IIIA/RDAS hardware simulation. The rationale for this decision was that if a worst-case analysis indicated that asynchronous interference would not significantly affect the ARTS-IIIA/RDAS performance a complete hardware simulation would not be necessary.

The two victim radars considered were the ASR-7 and ASR-8 interfaced with the ARTS-IIIA/RDAS processor. The interfering type radars considered included the ASR-7, ASR-8, AN/CPN-4, AN/FPS-90, and WSR-57. However, the analysis results are applicable to other type interfering radars in the 2.7 to 2.9 GHz band that have the same pulse width and pulse repetition frequency range.

Effect of Interference on the Probability of a Hit

The following is a discussion of the impact of interference on the RDAS rank order detection process which includes the rank quantizer and hit processor. A general equation is presented to determine the effect of interference on the probability of a hit (logical 1) when noise, desired signal, or clutter are in the range bin of interest. The effect of interference on the probability of a hit when noise, desired signal, or clutter is present in the range bin of interest is a function of the probability of a hit (logical 1) when noise only is present (P_{nl}), probability of a hit when noise and desired signal only are present (P_{sl}), and the probability of a hit when noise and clutter only are present (P_{cl}), respectively. For purposes of deriving a general equation for all the above conditions, a general term (P_l) will be used to represent a hit for P_{nl}, P_{sl}, and P_{cl}. The specific equation for P_{nl}, P_{sl}, and P_{cl} will then be derived in later subsections.

Asynchronous interfering radar video pulses can affect the probability of a hit at the hit processor output in two ways. First, an interfering radar pulse falling in the rank quantizer range bin of interest increases the probability of a hit (logical 1) being generated. Second, an interfering pulse falling in the rank quantizer comparison range bins decreases the probability of a hit. This is because an interference pulse falling in one or more of the comparison range bins lowers the probability of the voltage level in the range bin of interest exceeding the comparison range bin levels.

Both the above described interference mechanisms can be accounted for in a simple equation if it is assumed that the interfering signal-plus-noise level at the input to the RDAS is always greater than the target return signal-plus-noise level. If it is also assumed that the random arrival of interfering radar pulses in time can be described by a Poisson probability distribution, the effect of interference on the probability of a hit occurring is given by:

$$P_{i1} = [N(1-P_1)(1-e^{-X_1\nu})+P_1]e^{-NX_2\nu} \qquad (4-1)$$

where

P_{i1} = Probability of a logical 1 or hit being generated with interference present

P_1 = Probability of a logical 1 or hit being generated with no interference present

N = Indicator variable which takes into account the radar channel connected to the ARTS-IIIA/RDAS (N = 1 for Normal and N = 3 for MTI channel)

X_1 = Time interval that interfering radar pulse overlaps sample time of the rank quantizer range bin of interest, in seconds

X_2 = Time interval that interfering radar pulse overlaps the sample time of the rank quantizer comparison range bins, in seconds

ν = interfering pulse arrival rate, in pulses per second

The first factor in Equation 4-1 accounts for the probability of the interfering pulse falling in the rank quantizer range bin of interest. The second factor ($e^{-NX_2\nu}$) in the equation gives the probability of no interfering pulses falling in the comparison range bins since this is a necessary requirement for a logical 1 or hit to be generated. A detailed derivation of Equation 4-1 and justification of the assumptions is given in Appendix F.

The variable N in Equation 4-1 is set equal to 3 for the MTI channel because there is a high probability that one interfering pulse at the input of the double MTI canceller circuit (feed forward mode) input will produce three synchronous interfering pulses at its output. This implies that the probability of an interfering pulse falling into a given rank quantizer range bin is actually equal to the probability of it falling in that range bin for any one of three ACPs (present and two previous ACPs).

The values of X_1, and X_2, in Equation 4-1 depends on the interfering radar pulse width (τ_i) and victim radar range bin characteristics. In particular, the victim radar range bin width in time (RB_w), range bin sample

time (RB_s), and range bin hold time (RB_H), have to be considered. The value of X_1 for a given range of interfering radar pulse widths is defined by:

$$X_1 = \begin{cases} \tau_i + RB_s & \text{for } \tau_i < (3RB_w + RB_H) \\ 0 & \text{for } \tau_i > (3RB_w + RB_H) \end{cases} \qquad (4\text{-}2)$$

for the indicated interfering pulse width ranges. The value of X_2 also depends on the rank quantizer threshold setting. The value X_2 for a rank quantizer threshold (RQT) of 23 is given by:

$$X_{23} = \begin{cases} 22(\tau_i - RB_H) & \text{for } RB_H < \tau_i < (RB_w + RB_H) \\ 24RB_w & \text{for } \tau_i > (RB_w + RB_H) \end{cases} \qquad (4\text{-}3)$$

and for a RQT of 24 by:

$$X_{24} = \begin{cases} 24RB_w + 2(\tau_i - RB_H) & \text{for } RB_H < \tau_i < (RB_w + RB_H) \\ 26RB_w & \text{for } \tau_i > (RB_w + RB_H) \end{cases} \qquad (4\text{-}4)$$

Equations 4-2, 4-3, and 4-4 were derived graphically by assuming the interfering pulses to be perfectly square shaped and of constant amplitude.

Effect of Interference on Probability of False Alarm

A false alarm is defined as the declaration of a target when a target is not actually present. For a false target to be declared, a sequence of false hits (logical 1) due to noise or interference must first be generated by the hit processor in the same range bin in adjacent ACPs, and the target declaration hit and miss count threshold in the target detection software equaled or exceeded. Therefore, to analytically determine the probability of a false alarm, the probability of a false hit at the hit processor output for noise and interference must first be addressed and then be applied to the target declaration hit and miss count threshold. The last portion of this subsection discusses the operational interpretation of the probability of false alarm caused by noise and interference on the ARTS-IIIA.

Probability of False Target Hit Caused by Noise

The effects of noise (no interference present) on the probability of a false target hit (logical 1) at the hit processor output can be expressed as:

$$P_{n1} = \frac{J - RQT + 1}{J + 1} \qquad (4\text{-}5)$$

where

J = The number of rank quantizer comparison range bins (24)

RQT = Possible rank quantizer threshold settings (23 or 24)

For RQT=24, Equation 4-5 indicates a 0.04 probability that the noise level in the range bin of interest will exceed the noise level in all 24 comparison range bins. Similarly, for RQT=23, the equation gives a 0.08 probability that the noise level in the range bin of interest will exceed at least 23 of the 24 bins. Sufficient conditions for Equation 4-5 to hold are that the probability distributions for all of the bin samples be identical and independent. Under these statistical conditions, the rank order detection technique maintains a constant probability of false target hit for varying levels of noise and clutter. Equation 4-5 indicates this fact by being only a function of hardware parameters.

Probability of False Target Hits Caused by Interference

In order to determine the effect of interference on the probability of false target hit, the probability of a false target hit due to noise only must also be considered since the noise is always present in the RDAS. Therefore, the probability of a false target hit (logical 1) at the hit processor output due to interference (P_{i1}) is obtained by substituting Equation 4-5 (probability of target hit due to noise, P_{n1}) in Equation 4-1, which after algebraic simplification gives:

$$P_{i1} = \left\{ \frac{RQT}{J+1} [N(1-e^{-X_1 \nu})-1]+1 \right\} e^{-NX_2 \nu} \qquad (4-6)$$

For a rank quantizer threshold (RQT) of 23 Equation 4-6 becomes:

$$P_{i1}(23) = \left\{ 0.92 [N(1-e^{-X_1 \nu})-1]+1 \right\} e^{-NX_{23} \nu} \qquad (4-7)$$

and for RQT 24

$$P_{i1}(24) = \left\{ 0.96 [N(1-e^{-X_1 \nu})-1]+1 \right\} e^{-NX_{24} \nu} \qquad (4-8)$$

The X_1, X_{23}, and X_{24} are defined by Equations 4-2, 4-3, and 4-4, respectively, and evaluated for various interfering and victim radar combinations in TABLE 4-1. The probability of a false target hit as a function of the interfering signal pulse arrival rate (ν) was computed for each interfering and victim radar combination, using Equations 4-7 and 4-8, and the X_1, X_{23}, X_{24} values indicated in TABLE 4-1. The results of these calculations are indicated in Figures 4-8 through 4-15. The graphs in

TABLE 4-1

TIME INTERVALS THAT INTERFERING RADAR PULSES OVERLAP THE RANK QUANTIZER RANGE BIN SAMPLE TIMES FOR VARIOUS COMBINATIONS OF INTERFERING AND VICTIM RADARS

INTERFERING RADAR TYPE	INTERFERING PULSE WIDTH (τ_i) IN μs	VICTIM RADAR	X_1 IN μs (RQT = 23, 24)	X_{23} IN μs (RQT = 23)	X_{24} IN μs (RQT = 24)
ASR-7	0.833	ASR-7	0.989	8.030	15.730
ASR-8	0.600	ASR-7	0.756	2.904	15.264
AN/CPN-4	0.500	ASR-7	0.656	0.704	15.064
AN/FPS-90	2.000	ASR-7	2.156	15.000	16.250
WSR-57	4.000	ASR-7	0.000	15.000	16.250
ASR-7	0.833	ASR-8	0.999	11.726	12.142
ASR-8	0.600	ASR-8	0.766	6.600	11.808
AN/CPN-4	0.500	ASR-8	0.666	4.400	11.608
AN/FPS-90	2.000	ASR-8	0.000	11.208	12.142
WSR-57	4.000	ASR-8	0.000	11.208	12.142

NOTE: 1. VICTIM RADAR RANGE BIN CHARACTERISTICS
ASR-7 : RB_W = 0.625 μs, RB_S = 0.156 μs, RB_H = 0.468 μs
ASR-8 : RB_W = 0.467 μs, RB_S = 0.166 μs, RB_H = 0.300 μs

2. RQT = RANK QUANTIZER THRESHOLD

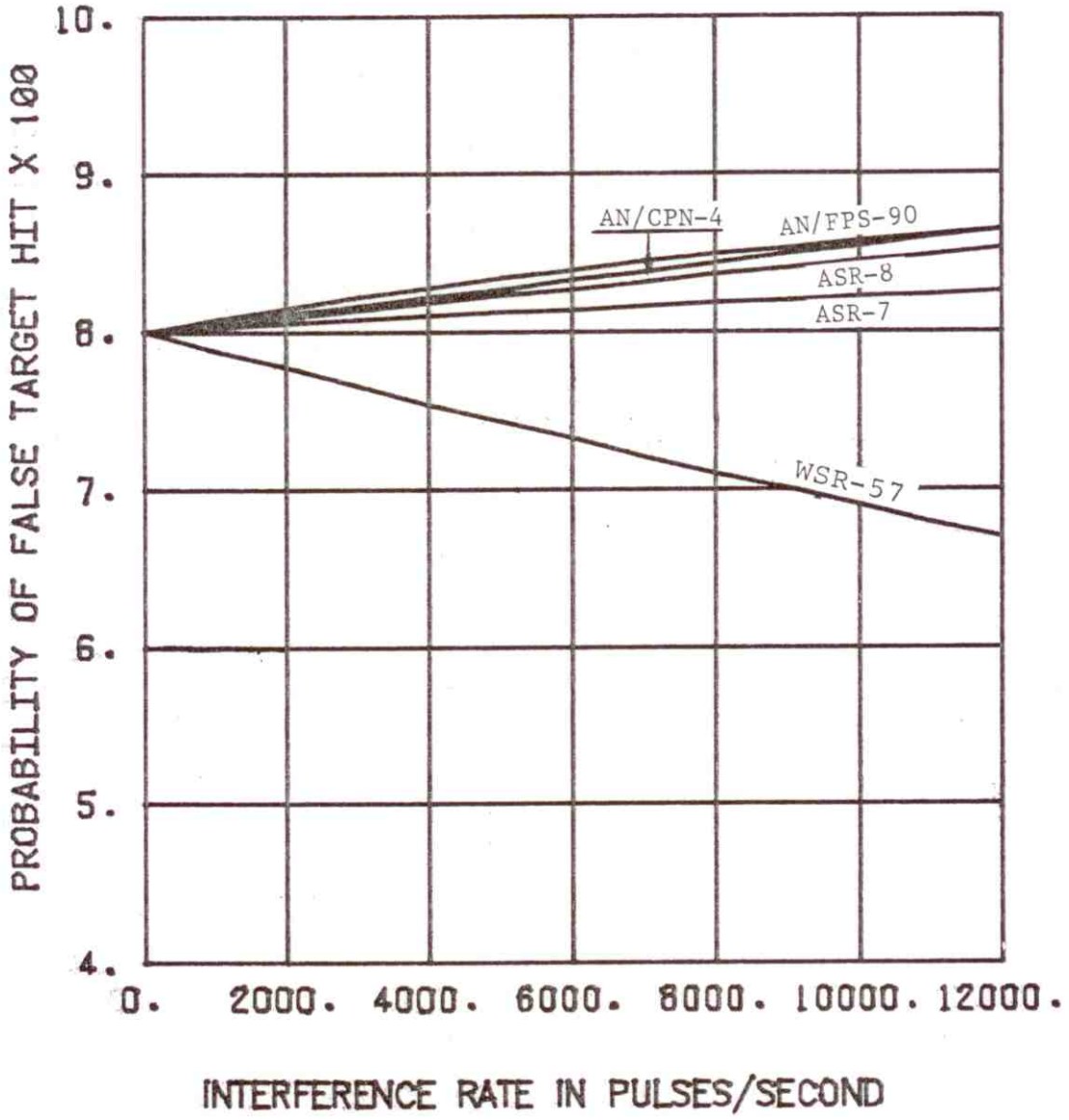

Figure 4-8. ARTS-IIIA/RDAS Probability of False Target Hit Versus Rate of Received Interference (ASR-7 Victim Radar, Normal Channel, Rank Quantizer Threshold 23)

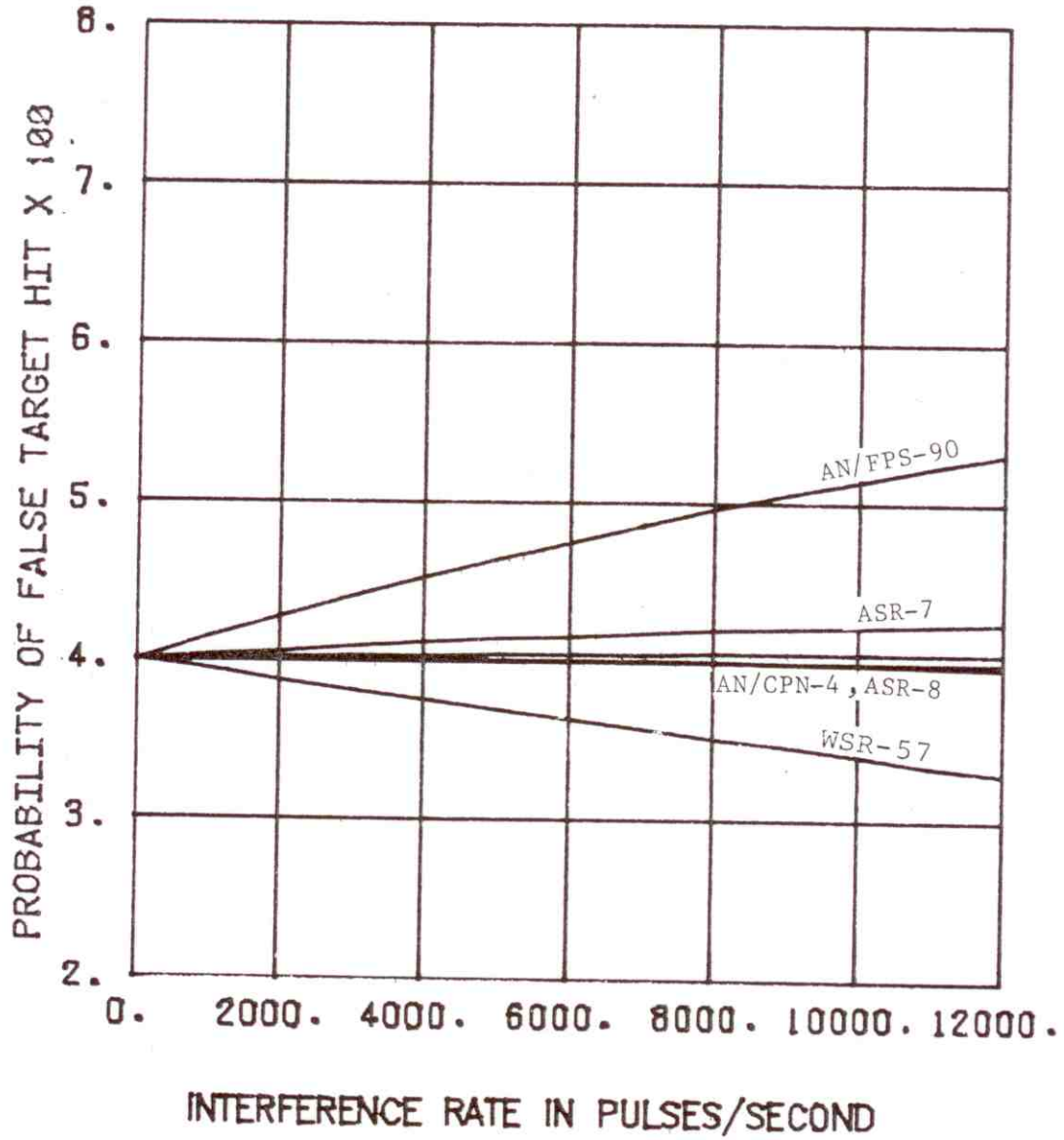

Figure 4-9. ARTS-IIIA/RDAS Probability of False Target Hit Versus Rate of Received Interference (ASR-7 Victim Radar, Normal Channel, Rank Quantizer Threshold 24)

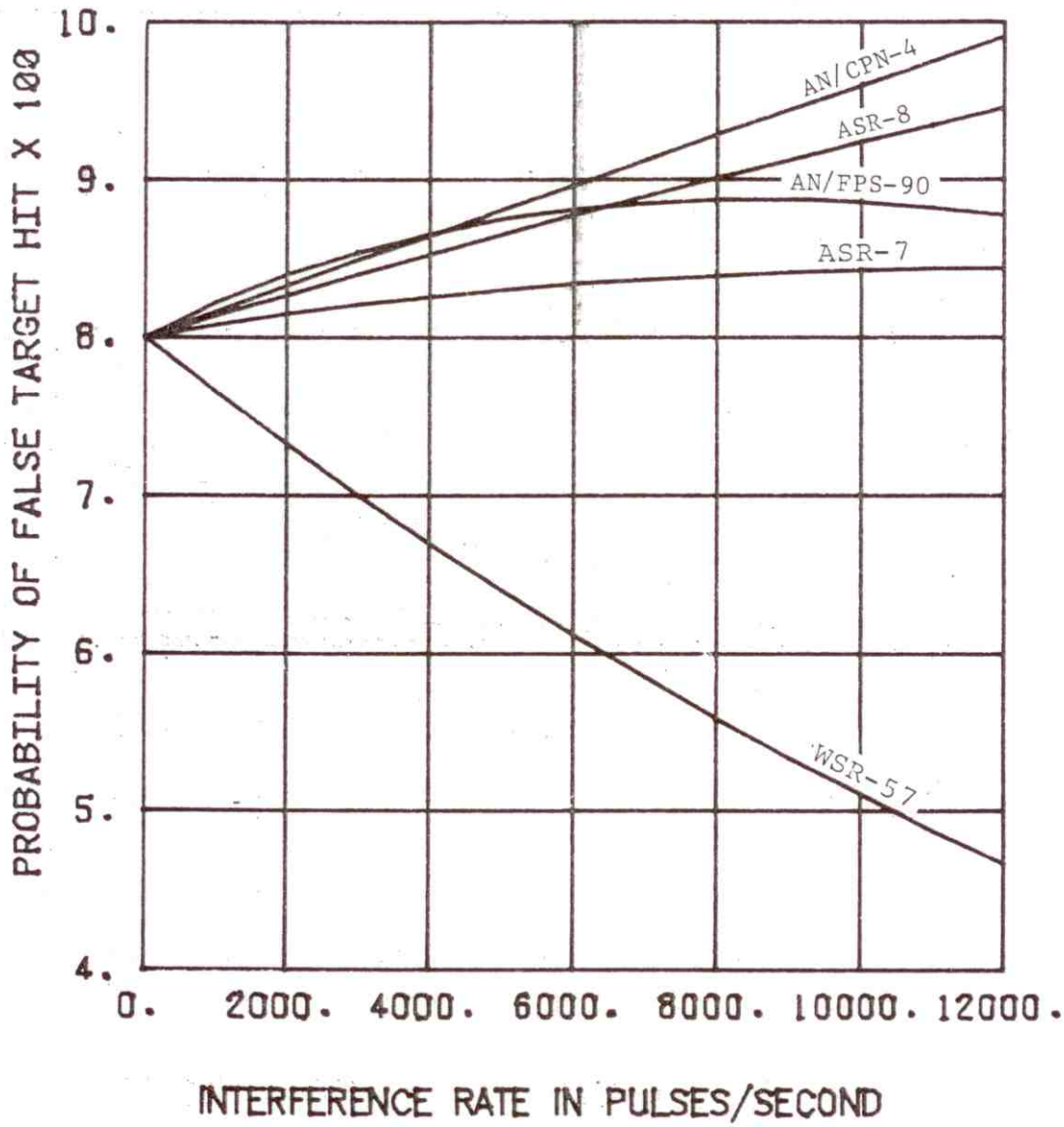

Figure 4-10. ARTS-IIIA/RDAS Probability of False Target Hit Versus Rate of Received Interference (ASR-7 Victim Radar, MTI Channel, Rank Quantizer Threshold 23)

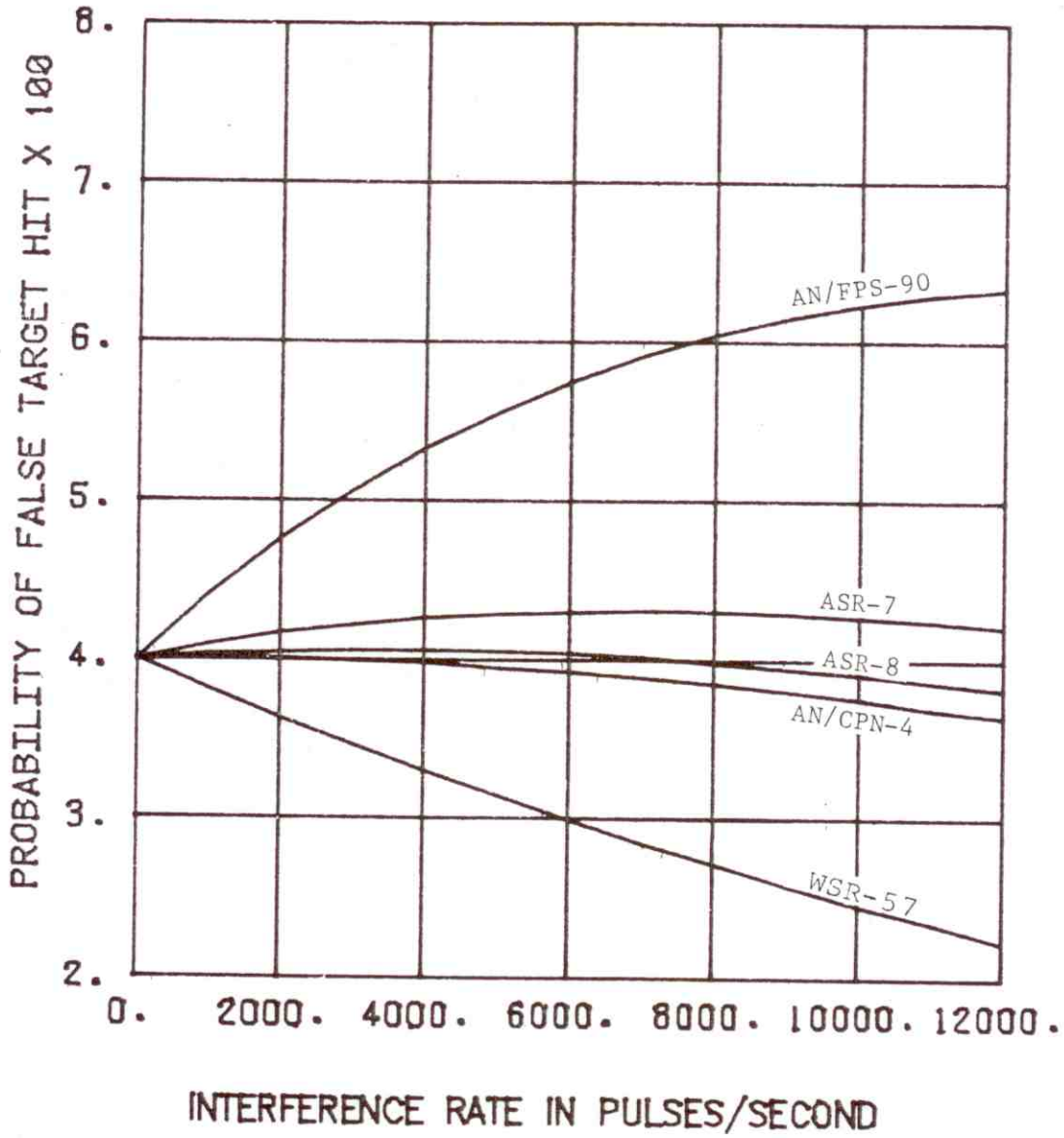

Figure 4-11. ARTS-IIIA/RDAS Probability of False Target Hit Versus Rate of Received Interference (ASR-7 Victim Radar, MTI Channel, Rank Quantizer Threshold 24)

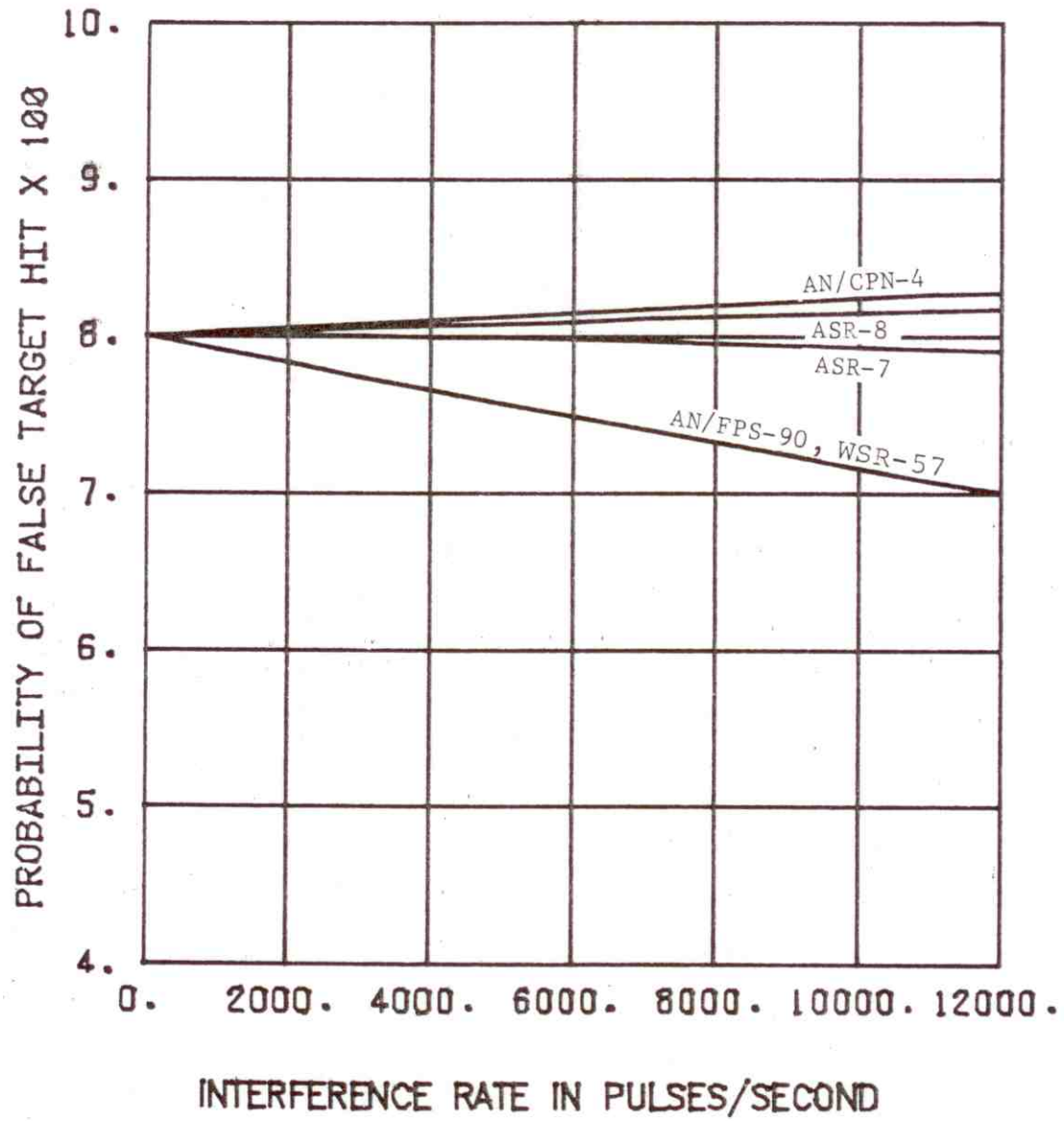

Figure 4-12. ARTS-IIIA/RDAS Probability of False Target Hit Versus Rate of Received Interference (ASR-8 Victim Radar, Normal Channel, Rank Quantizer Threshold 23)

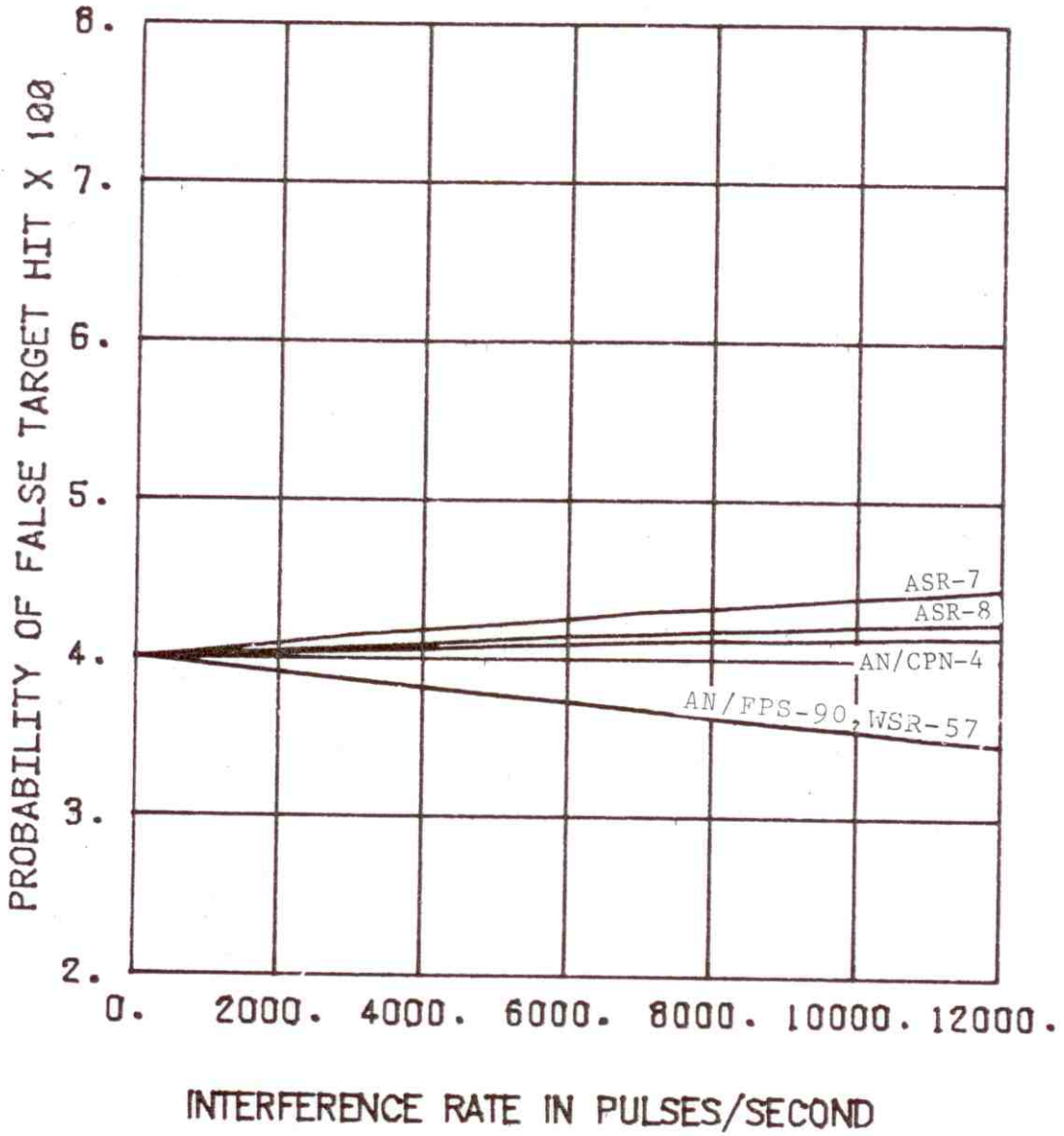

Figure 4-13. ARTS-IIIA/RDAS Probability of False Target Hit Versus Rate of Received Interference (ASR-8 Victim Radar, Normal Channel, Rank Quantizer Threshold 24)

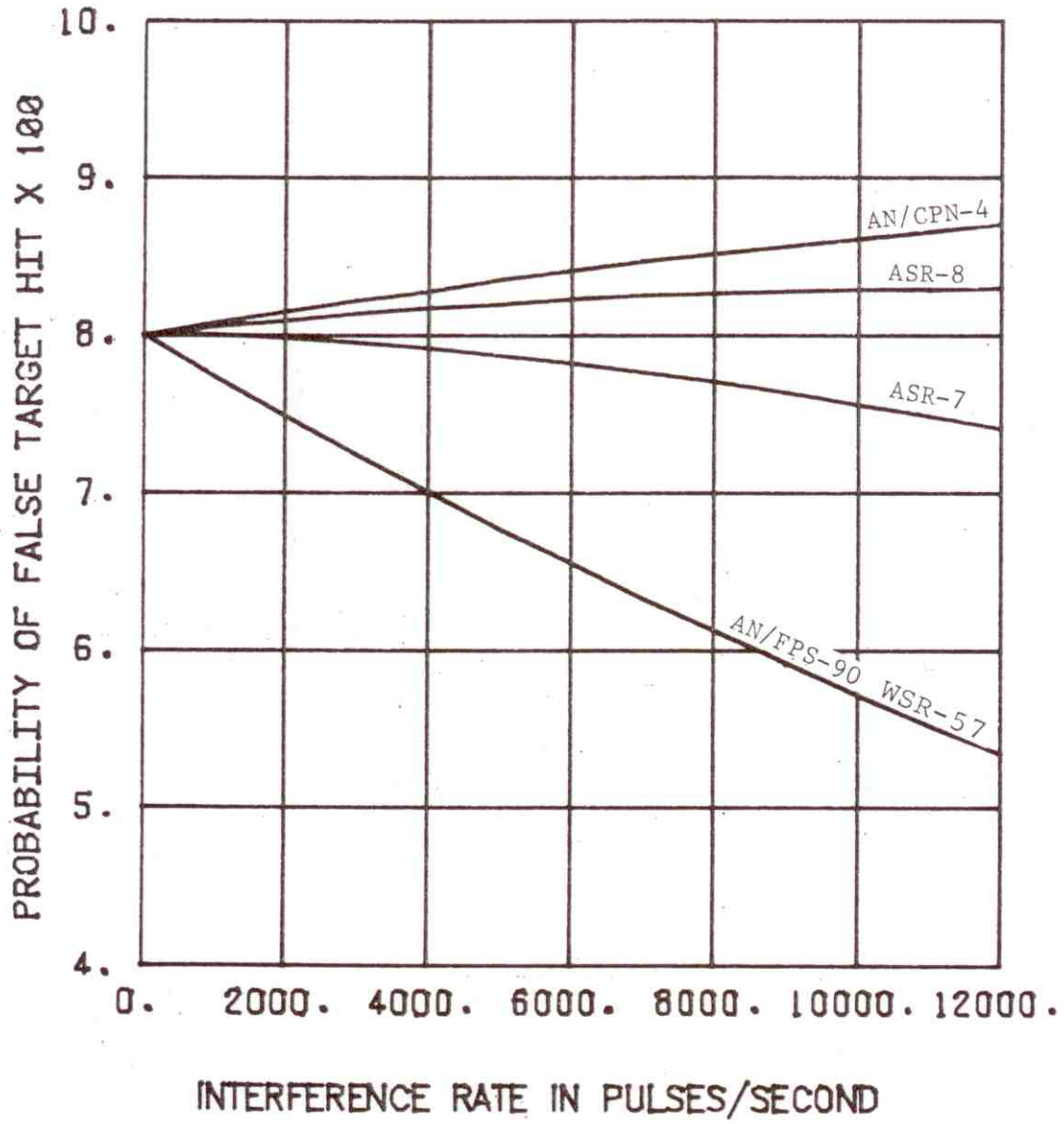

Figure 4-14. ARTS-IIIA/RDAS Probability of False Target Hit Versus Rate of Received Interference (ASR-8 Victim Radar, MTI Channel, Rank Quantizer Threshold 23)

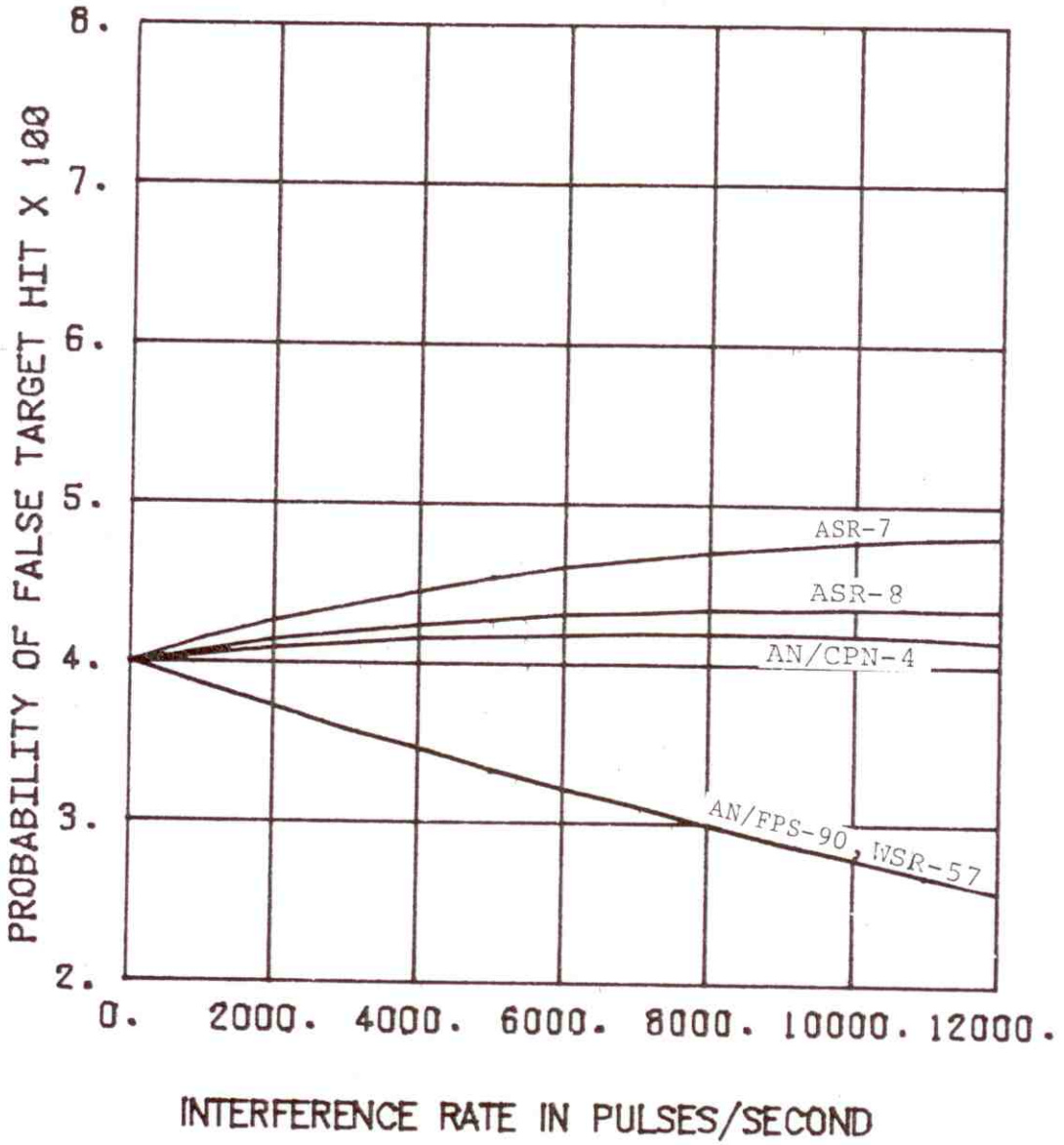

Figure 4-15. ARTS-IIIA/RDAS Probability of False Target Hit Versus Rate of Received Interference (ASR-8 Victim Radar, MTI Channel, Rank Quantizer Threshold 24)

Figures 4-8 through 4-11 are for the ARTS-IIIA/RDAS interfaced to the ASR-7, and Figures 4-12 through 4-15 the ARTS-IIIA interfaced to the ASR-8. In addition, the graphs consider the ARTS-IIIA/RDAS connected to both the normal and MTI channel. The family of curves on each graph represent various interfering radar types. However, the curves are applicable to other interfering radar types in the 2.7-2.9 GHz band that have the same pulse widths. The interfering radar pulse widths corresponding to the various radar types is given in Appendix G. The 4.0 μs pulse width mode of the WSR-57 was used for calculation of the curves. The even numbered figures are for RQT=23 and the odd number for a RQT=24. The interference rate of zero value on each curve represents the probability of a false target hit due to only noise. It is evident from the graphs that the probability of false target hit is more affected for a rank quantizer threshold setting of 24 than 23. In addition, interference has a greater impact on the RDAS when connected to the MTI than the normal channel. This is due to the generation of several synchronous interfering pulses by the MTI cancellers in the primary radar (see Section 3 and Appendix C).

The data represented by the curves in Figures 4-8 through 4-15 were reduced to the form shown in TABLES 4-2 through 4-5 to indicate the effect of a particular number and type of interfering radars on the probability of false target hit. TABLES 4-2 and 4-3 represent data for the ARTS-IIIA/RDAS interfaced to an ARS-7 radar that is receiving interference from one and three radars, respectively. Similarly, TABLES 4-4 and 4-5 give the probability of false target hit when the ARTS-IIIA/RDAS is connected to an ASR-8 victim radar. The interfering pulse arrival rate (ν) in TABLES 4-2 and 4-4 are simply equal to the interfering radar average pulse repetition frequency (PRF), and in TABLES 4-3 and 4-5, 3 times the interfering radar PRF.

Probability of False Alarm Caused by Interference

The decision in regard to the presence of a target is accomplished by the target detection software functions shown in Figure 4-5. The details of this target detection processing is given in the RDAS description section of this report. Basically, a count of hits (logical 1's) and consecutive misses (logical 0's) are maintained in azimuth for a given range bin. If the consecutive miss count equals or exceeds a miss count threshold and the hit count equals or exceeds a hit count threshold, a target is declared.

A computer program was written to calculate the probability of false alarm as a function of false target hit probability . The program employs a combination of simulation and analytical methods. The details of this program are given in Appendix F, and the results of the calculations are shown in Figure 4-16. The probability of false alarm versus probability of false target hit for various combinations of detection parameters is shown. It is evident from the curves in Figure 4-16 that holding the miss count threshold constant and decreasing the hit count threshold increases the probability of false alarm. This result is reasonable when one considers that a sequence of hits and misses is a set of Bernoulli trials. Since the